Chapter 05: Welding and Characterization of Aluminium Matrix Composite

5.1 Preamble

The present chapter discusses joining of Aluminium Matrix Composites (AMC) using a solid state joining process i.e. Friction Stir Welding (FSW). As state earlier, the joining of AMC using conventional welding process results in the formation of a deleterious phase which ultimately degrades the mechanical and metallurgical properties of the weld joint. Formation of deleterious phase can be avoided if welding of AMC occurs at a temperature lower than its melting point. Due to the same, solid state joining process FSW has been considered for joining AMC. Furthermore, the chapter discusses several joint characteristics such as macrostructure, microstructure, tensile strength and microhardness of the welded composites.

5.2 Friction stir welding of AMC

FSW was performed on the vertical milling machine to joining as-cast composites. H13 tool having cylindrical taper threaded pin was used for performing FSW. The dimension of the tool was the same, as mentioned in Figure 4.4. The as-cast plates were having some irregular surface and poor surface finishing. These asperities along with poor surface finishing were resolved by doing machining. For FSW, the composites plates were having a width of 50 mm, length of 100 mm and thickness of 6 mm. The as-cast plates were held in the same manner as shown in Figure 4.3. Welding of all composites was accomplished by maintaining rotational speed of 270 rpm, welding speed of 78 mm/min and tool tilt angle of 2°.

5.3 Characterization of welded composites

The welded composites were evaluated for microstructure, microhardness and tensile strength. For evaluating these properties, the specimens from welded plates were cut as per the schematic shown in Figure 5.1. Microstructural characteristics were investigated using Optical Microscope (OM) and Scanning Electron Microscope (SEM). The cross-section of the specimen was polished according to the standard metallurgical

procedure. For etchant, Keller's reagent was prepared by mixing distilled water, nitric acid, hydrochloric acid and hydrofluoric acid in proportionate quantity. Keller's reagent was then applied on the polished surface of the specimen at room temperature and was dried out before microstructure examination.

For measurement of microhardness, the indentation was performed at the mid thickness (i.e. 3 mm from top surface) of the weld cross-section. Microhardness test was performed for a load of 300 gf with a dwell period of 10 sec and hardness was measure in Vickers Hardness Number (VHN). Lastly, the specimens for the tensile test were prepared as per ASTM E08 standards. The specimen required for the tensile test were cut using wire cut Electrical Discharge Machining (EDM) as per the dimension shown in Figure 5.2. To get a clear and better understanding of tensile strength, three different specimens were taken from each composition and the final tensile strength was considered as the average of three values. The tensile test was performed on Universal Testing Machine (UTM) under a controlled strain rate of 1 mm/min.

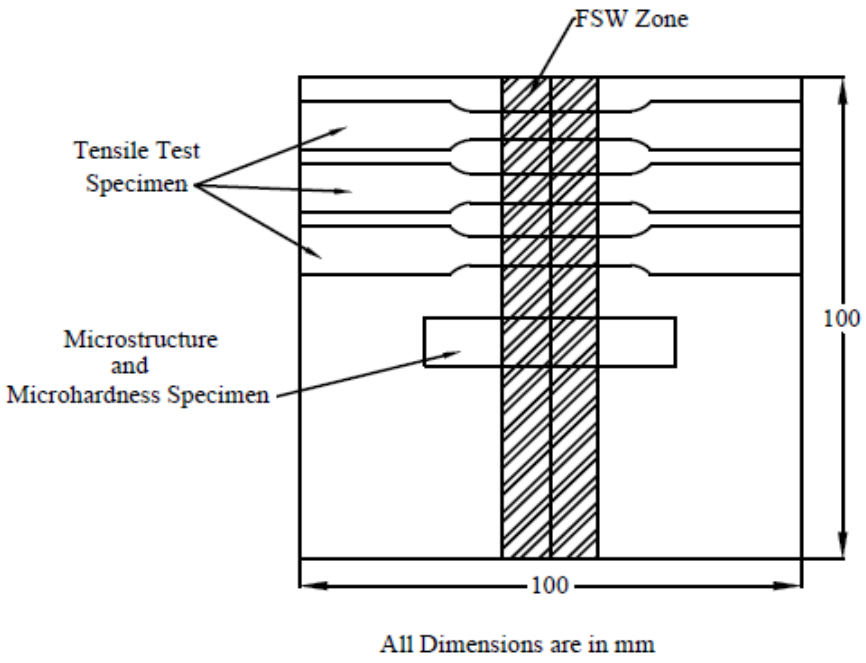

Figure 5.1 Schematic showing the specimens taken from welded plates

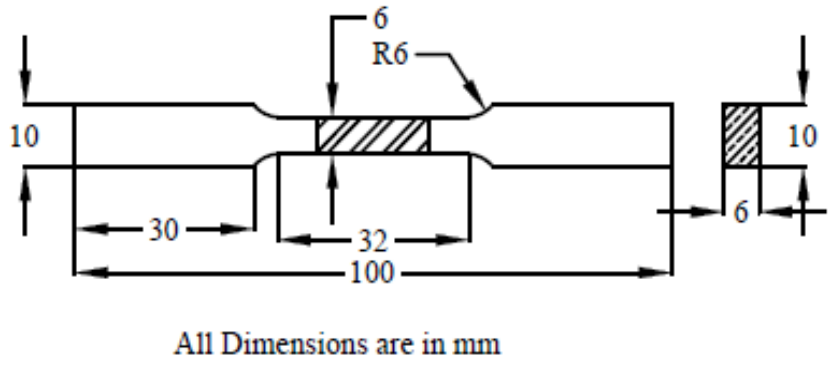

Figure 5.2 Schematic showing dimensions of tensile specimens

5.4 Macrostructure Investigation

The macrostructure of different welded composites is shown in Figure 5.3 (a) - (c). From Figure 5.3 (a) - (c), it can be observed that the obtained macrostructure of all welded composites was free from welding defects such as void, porosity, pinhole and tunnel defects. As marked in Figure 5.3 (a), it can be observed that the macrostructure was found to have few particle rich regions in which the content of SiC particles was higher. On the other side, the macrostructure of AA 2014 + 10% SiC was found to have a homogeneous distribution of reinforcement particles in the weld zone. Also, the macrostructure presented in Figure 5.3 (b) didn't revealed any particle rich regions or agglomeration of SiC particles. However, the macrostructure of welded AA 2014 + 15% SiC reveal agglomeration of reinforcement particles at the bottom/root of the welded joint. It should be noted that a higher weight percent of reinforcement particles will offer higher resistance to the rotating tool. This will result in higher friction between the rotating tool and workpiece. As a result of this, the macrostructure of welded AA 2014 + 15% SiC revealed signs of generation of excessive frictional heat.

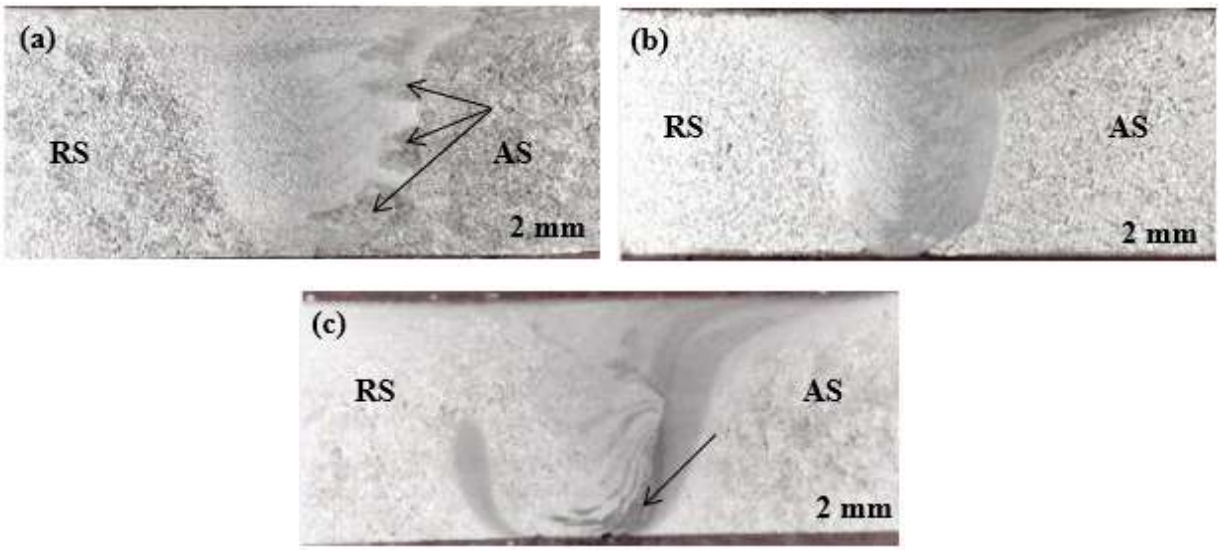

Figure 5.3 Macrostructure of friction stir welded (a) AA 2014 + 5% SiC, (b) AA 2014 + 10% SiC and (c) AA 2014 + 15% SiC

5.5 Microstructure Investigation

The microstructure from the as-cast region observed using an OM is shown in Figure 5.4. As a result of stir casting, the manufactured composites are characterized by a dendritic like structure. The discontinuous reinforcement phase, i.e. particulates of SiC having non-uniform size and shape was found to disperse randomly within the matrix of aluminium alloy. It can also be observed that an increase in the weight percent of reinforcement particles tends to increase the dendritic structure. During the solidification, the small nuclei formed during the nucleation process will try to block each other mechanically, and this blocking will result in the formation of dendrites. It should be noted that for a higher weight percent of reinforcement particles, a higher number of nuclei will be generated. This will ultimately increase the dendrites in solidified composites. Due to the lower weight percent of reinforcement particles, the microstructure of AA 2014 + 5% SiC presented in Figure 5.4 (a) was found to have particle free regions. However, with the increase in weight percent of reinforcement particles, the particle free regions in microstructure were found to reduce. Earlier it has been reported that an increase in the weight percent of reinforcement particles beyond a certain limit results in the formation of clusters of reinforcement particles. Similar to this, AA 2014 + 15% SiC was found to have cluster/agglomeration of reinforcement particles and the same has been shown in Figure 5.4 (c). Thus, it can be said that an increase in the weight percent of reinforcement particles will tend to reduce the particle free region,

whereas increases the possibility of the formation of clusters/agglomeration of reinforcement particles.

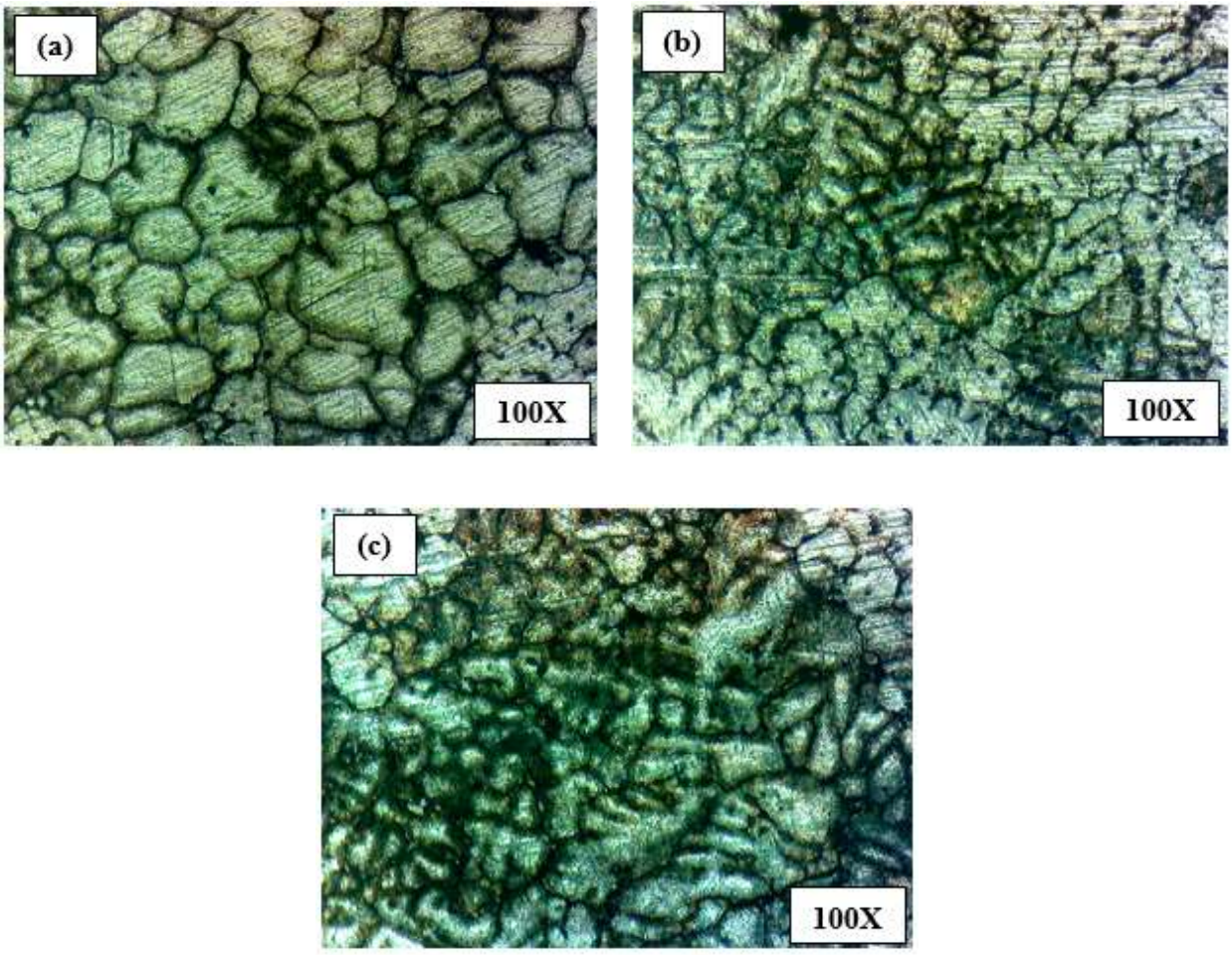

Figure 5.4 As-cast region of (a) AA 2014 + 5% SiC, (b) AA 2014 + 10% SiC and (c) AA 2014 + 15% SiC observed using OM

To get a clear idea about the presence of SiC particles in the aluminium matrix, microstructure analysis was performed using SEM and obtained images are presented in Figure 5.5. In Figure 5.5 (a) – (c), presence of SiC particles in the matrix of AA 2014 can be observed and the same has been marked by an arrow. Good interfacial bonding between reinforcement particles and matrix can be observed. The SiC particles which were embedded in the matrix of AA 2014 were found to have an irregular shape and size. It should be noted that the stirring action by the mechanical stirrer tends to break the reinforcement particles. Also the mechanical stirrer distributes those broken particles in the aluminium matrix. Apart from this, no interfacial reaction between matrix and reinforcement phase was observed as the grain boundaries were clear and no deleterious

phase was present. Figure 5.5 (a) also highlights the particles free region, which was generated as a result of the lower weight percent of reinforcement particles. Along with this, Figure 5.5 (c) demonstrates the agglomeration of reinforcement particles which was generated as a result of a higher weight percent of SiC particles. However, the microstructure of AA 2014 + 10% SiC didn't reveal any particle free region or agglomeration of reinforcement particles. From Figure 5.5 (b), the homogenous distribution of SiC particles in the matrix of AA 2014 can be observed.

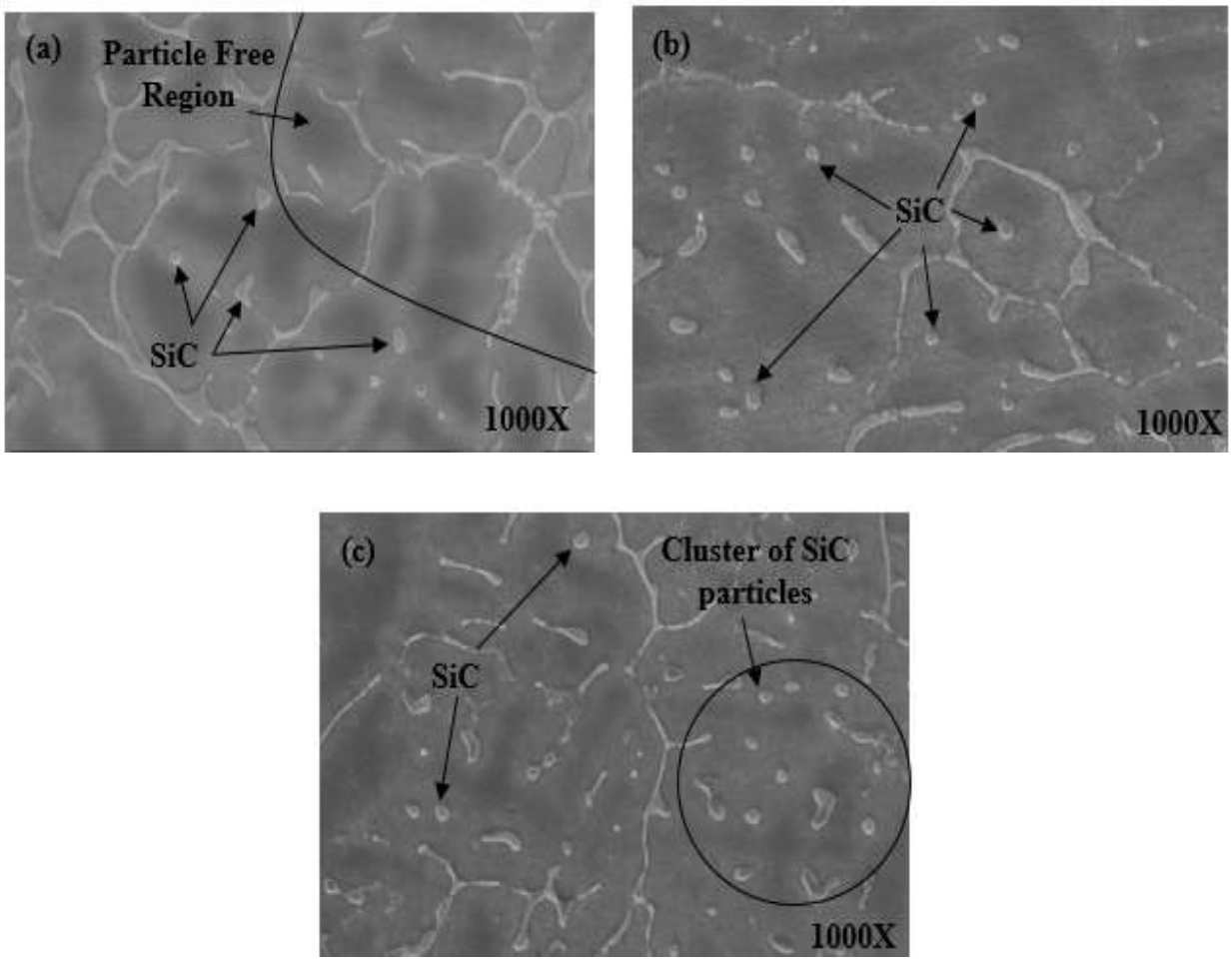

Figure 5.5 As-cast region of (a) AA 2014 + 5% SiC, (b) AA 2014 + 10% SiC and (c) AA 2014 + 15% SiC

FSW tends to create three different zones in the weld area which are known as Heat Affected Zone (HAZ), Thermo-Mechanically Affected Zone (TMAZ) and Weld Nugget (WN). The formation of these aforementioned zones has been discussed previously. Material under HAZ will not undergo the plastic deformation caused due to the FSW tool and thus, the microstructure of HAZ will be similar to that of as-cast composites. The

microstructure images of HAZ of all welded composites are presented in Figure 5.6. From Figure 5.6 (a) – (c) it can be observed that the microstructure of HAZ is almost similar to the microstructure of as-cast composites. However, the noteworthy point over here is that the resulting microstructure of HAZ was found to have voids. While comparing Figure 5.6 (a) – (c) it can be said that the void formation in the HAZ increases with the increase in the weight percent of reinforcement particles. It will not be wrong to comment that the defects observed in HAZ are the casting defects, as the material under this zone will only be experiencing the thermal history and will not undergo any kind of deformation.

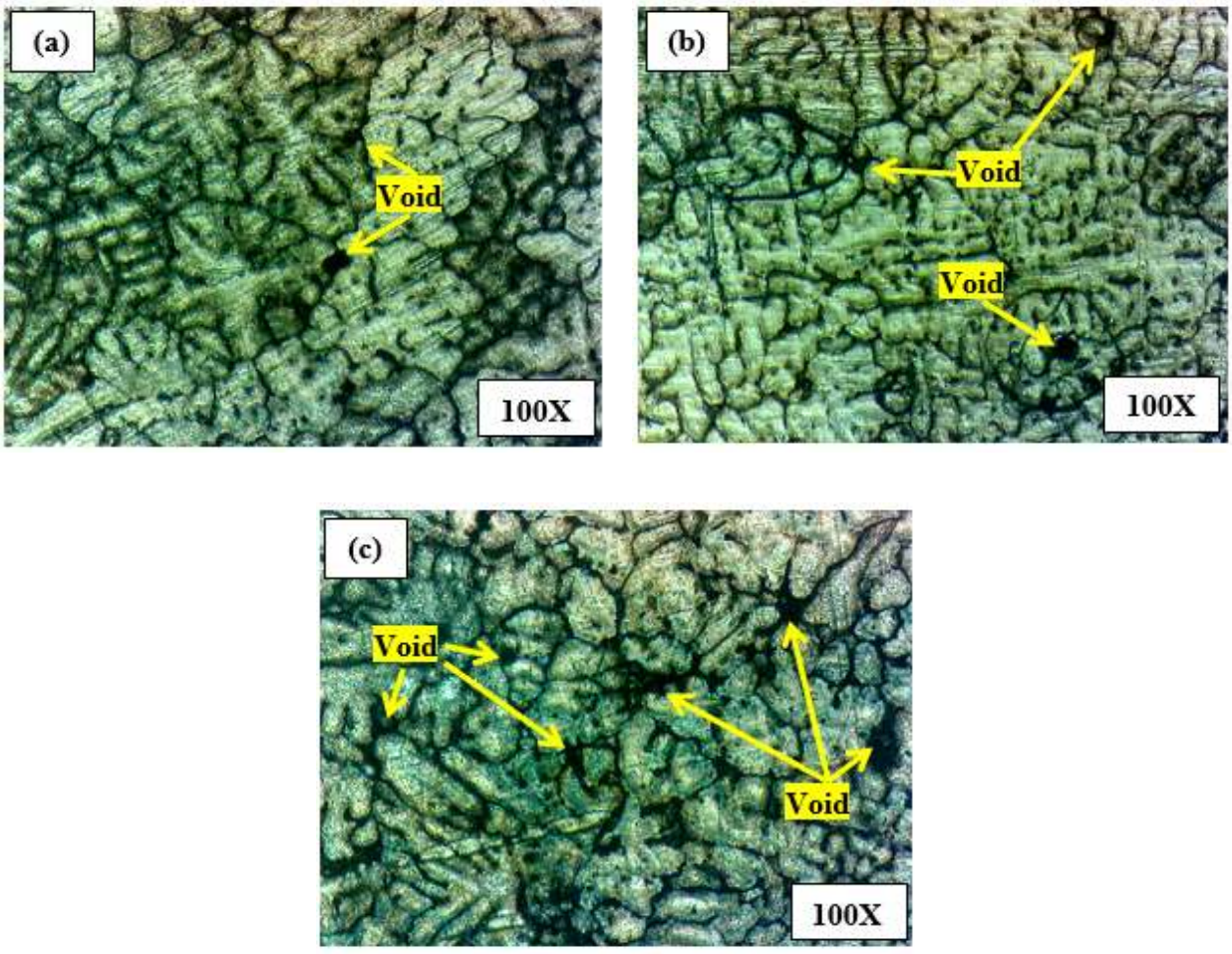

Figure 5.6 HAZ of (a) AA 2014 + 5% SiC, (b) AA 2014 + 10% SiC and (c) AA 2014 + 15% SiC observed using OM

As the name suggests, the TMAZ is the zone in which the material will experience both thermal histories and plastic deformation. But it should be noted that the thermal histories and plastic deformation experienced by the material under this zone will be

comparatively lower. Due to the same, the material under this zone will not experience dynamic recrystallization. The microstructure of TMAZ is presented in Figure 5.7. While comparing Figure 5.6 (a) – (c) with Figure 5.7 (a) – (c), it can be said that the microstructure of TMAZ is denser compared to HAZ. From Figure 5.7 (a) – (c) it can be observed that AA 2014 + 5% SiC and AA 2014 + 10% SiC were having lower welding defects. However, TMAZ of AA 2014 + 15% SiC was found to have comparatively higher welding defects such as voids and porosity. Thus, it was found that the defects in TMAZ tend to increase with the increase in weight percent of reinforcement particles. It should be noted that the presence of a higher weight percent of reinforcement will restrict the flow of plasticized material during the welding process and thus, as a result of lack of stirring, these welding defects such as porosity and voids are generated in AA 2014 + 15% SiC.

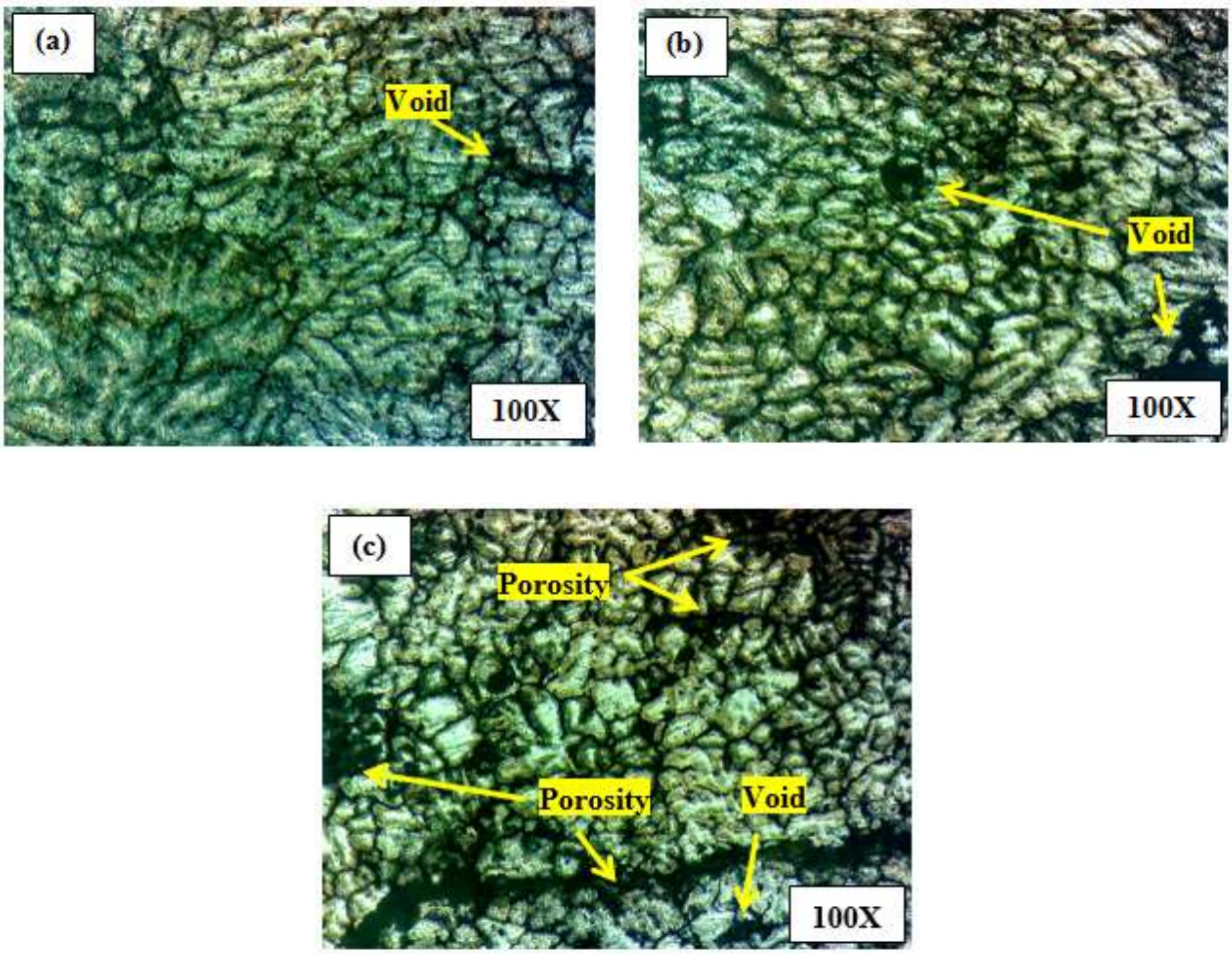

Figure 5.7 TMAZ of (a) AA 2014 + 5% SiC, (b) AA 2014 + 10% SiC and (c) AA 2014 + 15% SiC observed using OM

To get a clear idea about the variation in the microstructure of various zones, images captured using SEM has been shown in Figure 5.8. The microstructure shown in Figure 5.8 marks the boundaries between HAZ, TMAZ and WN. From the same, it can be observed that the TMAZ is characterized by elongated grains which are oriented towards the WN. It should also be noted that AA 2014 + 10% SiC was having higher width of TMAZ compared to the other two compositions. A noteworthy point over here is that all the zones were characterized by the presence of SiC particles. However, the size of SiC particles was comparatively smaller in the WN. While comparing the microstructure of the WN with the other two zones, substantial grain refinement along with dynamic recrystallization can be observed.

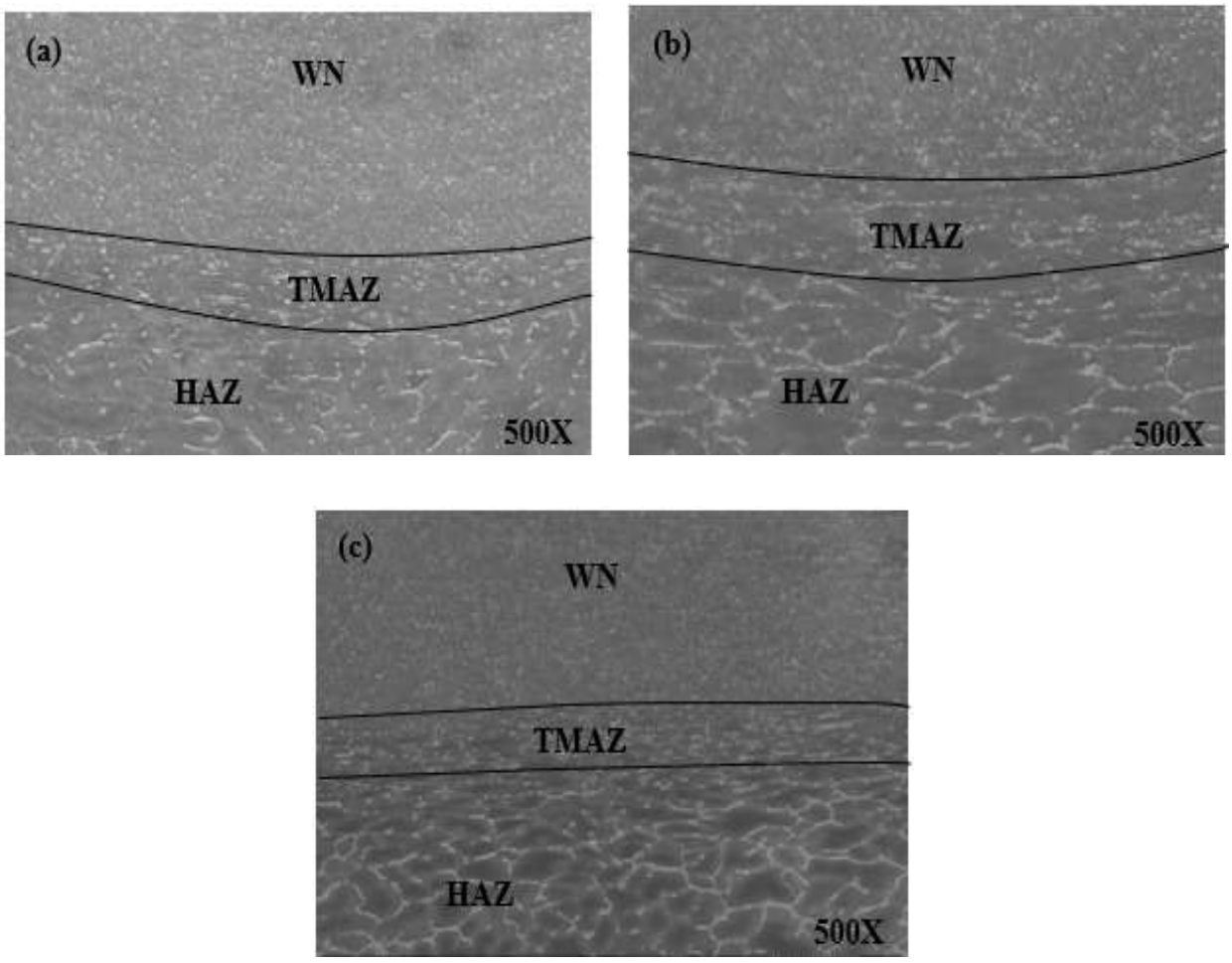

Figure 5.8 Transition zone of (a) AA 2014 + 5% SiC, (b) AA 2014 + 10% SiC and (c) AA 2014 + 15% SiC captured using SEM

WN is the zone that was previously occupied by the pin of the FSW tool. The material under this zone will be subjected to a comparatively higher temperature and higher plastic deformation. This high temperature and extensive plastic deformation will result in recrystallization. Due to the same, the microstructure of the WN is characterized by fine and equiaxed grains. From Figure 5.9 (a) – (c), the presence of SiC particles in the WN of all three composites can be observed. While comparing Figure 5.5 with Figure 5.9, a reduction in the size of SiC particles can be observed. During the FSW, the rotating tool tends to break the SiC particles present in the vicinity of a pin and homogeneously distributes those broken particles in the WN. Thus, the FSW tool contributes towards (i) grain refinement and (ii) homogenous distribution of reinforcement particles in the WN. It should also be noted that AA 2014 + 5% SiC and AA 2014 + 10% SiC was found to have a marginal reduction in the size of SiC particles present in the weld nugget. However, AA 2014 + 15% SiC was found to have several larger size SiC particles present in the WN. An increase in weight percent of ceramic particles will oppose the stirring action of the rotating tool. Due to the same, the stirring tool will fail to break the SiC particles present in the vicinity of a pin. Also, the higher weight percent of reinforcement particles will restrict the movement of the plasticized material. Due to the same, the distribution of SiC particles will be affected. Owing to this, a particle free region and comparatively larger size of SiC particles were observed in the WN of AA 2014 + 15% SiC. As shown in Figure 5.10 (a) – (c), some of the regions in the WN were found to have few welding defects especially voids. However, defects observed in the WN were lower in comparison to the defects observed in the TMAZ and HAZ. From Figure 5.10 (a), a continuous band having a comparatively finer grain size can be observed in the WN of AA 2014 + 5% SiC. However, the WN of the other two composites didn’t reveal any such band.

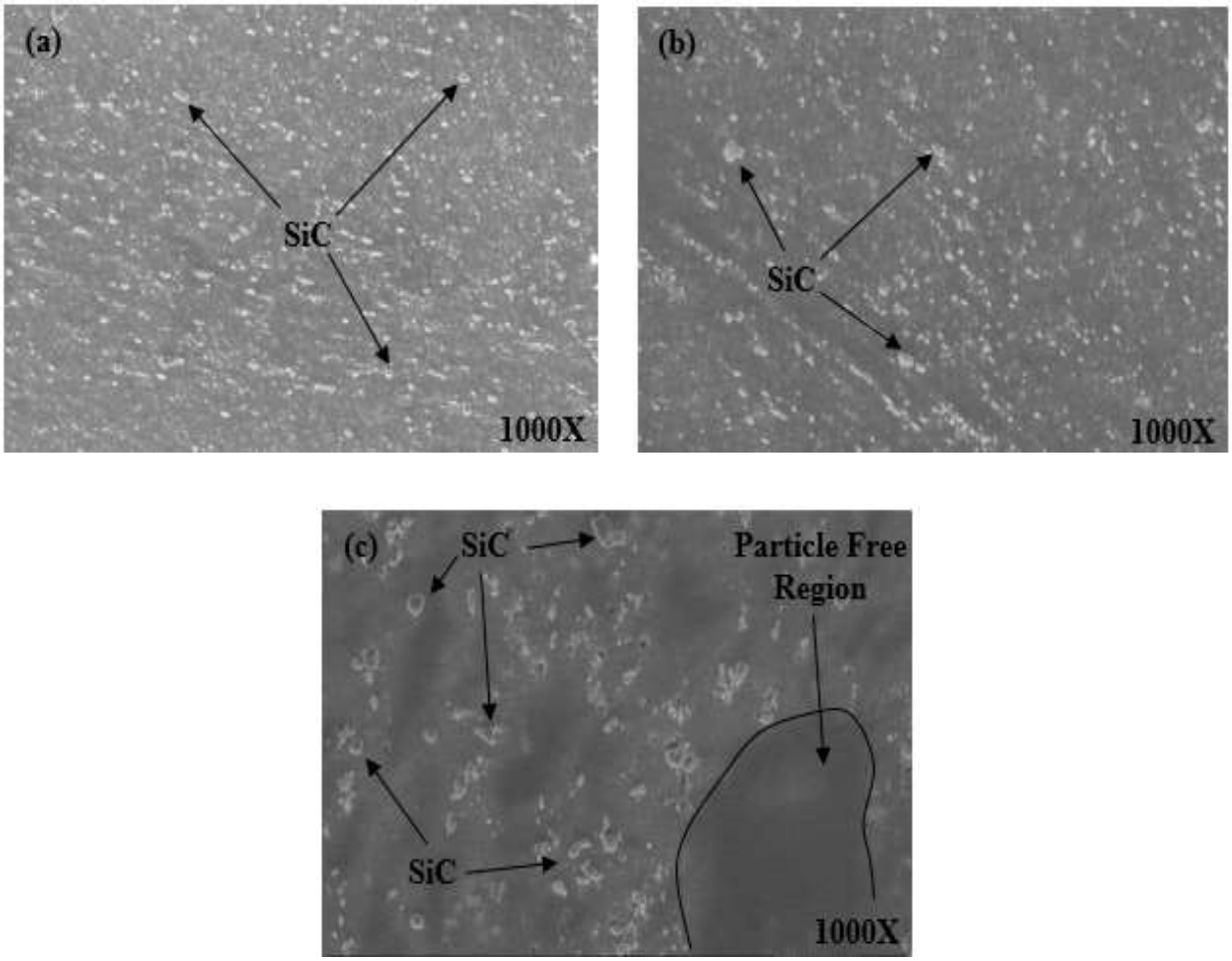

Figure 5.9 WN of (a) AA 2014 + 5% SiC, (b) AA 2014 + 10% SiC and (c) AA 2014 + 15% SiC captured using SEM

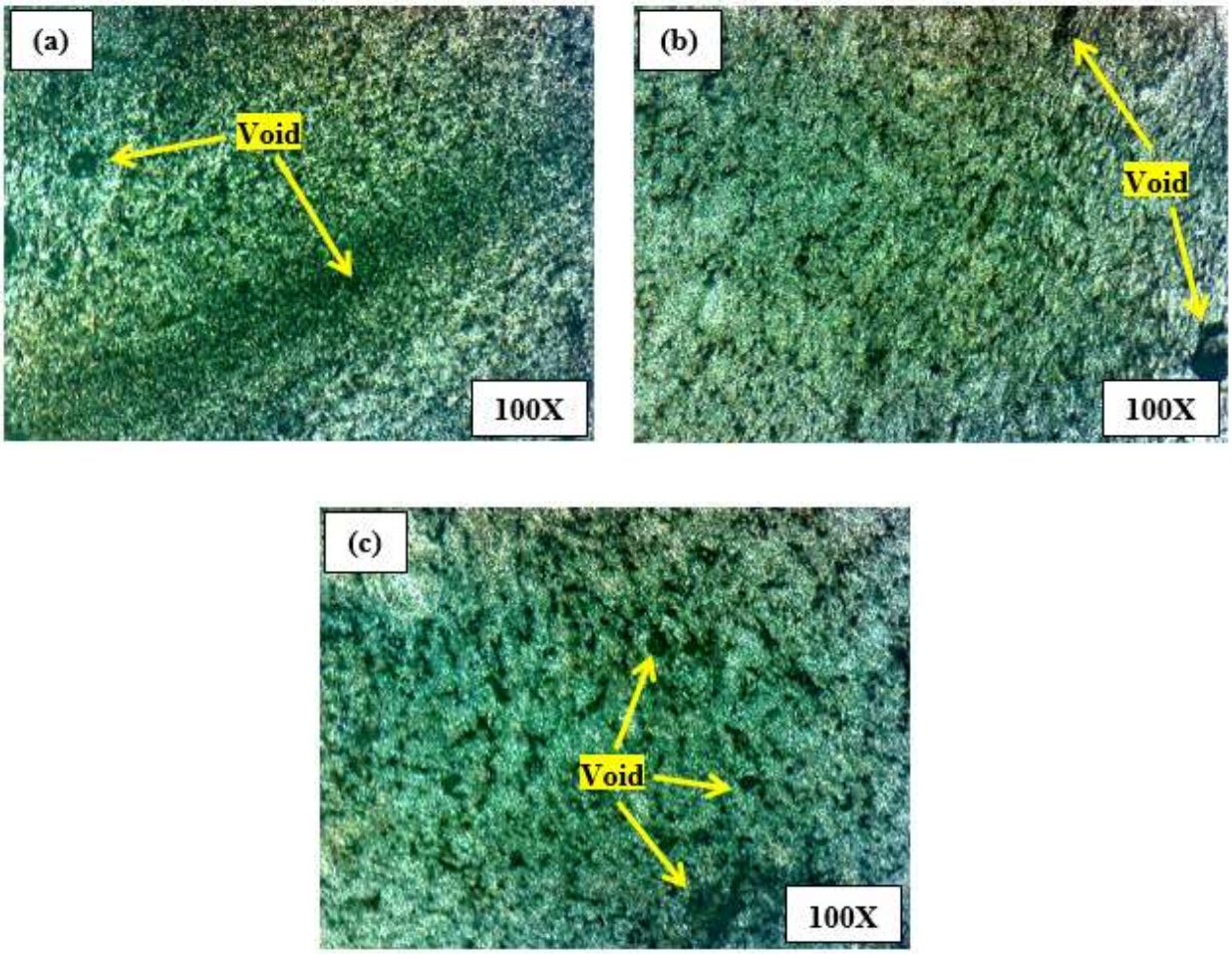

Figure 5.10 Defects in WN (a) AA 2014 + 5% SiC, (b) AA 2014 + 10% SiC and (c) AA 2014 + 15% SiC captured using OM

5.6 Tensile Strength of Welded Composite

The average tensile strength of as-cast and welded composites is presented in Figure 5.11. Compared to as-cast composites, substantial reduction in tensile strength of welded composites can be observed. However, the reduced tensile strength of welded joint still follows the same trend line which was previously observed in as-cast composites. Tensile strength of welded composites was found to increase with an increase in weight percent of reinforcement particles from 5% to 10%. Whereas, further increase in weight percent of reinforcement particles tends to degrade the tensile strength of the welded composite. In comparison to as-cast composites, the tensile strength of welded composites reduces by 31.16%, 22.90% and 18.85% for AA 2014 + 5% SiC, AA 2014 + 10% SiC and AA 2014 + 15% SiC respectively. Thus, it can be said that the difference between the tensile

strength of as-cast and welded composites reduces with the increase in the weight percent of reinforcement particles. The lower ultimate tensile strength of the welded composite is attributed to the over-ageing of AA 2014 induced due to frictional heat generated during the welding process. The over-ageing of aluminium alloy 2014 will lead to a coarsening of the intermetallic precipitates in the weld zone (Ceschini, Boromei, Minak, Morri, & Tarterini, 2007b). During over-ageing, the precipitates transform from coherent or semi-coherent to incoherent. This transformation will change the mechanics of plastic deformation from Ashby's to Orowan's mechanism (Dieter G., 1988). Also, the transformation will significantly reduce the ultimate tensile strength of the welded joint and correspondingly increases the strain hardening exponent. The strain hardening exponent (n) was calculated using the relation shown in equation 1. The calculated values of strain hardening exponent for as-cast AA 2014 + 5% SiC, AA 2014 + 10% SiC and AA 2014 + 15% SiC are 0.22, 0.19 and 0.21 respectively. Whereas, the same index n for welded composites are 0.30, 0.28 and 0.25 respectively, indicating a higher degree of strain hardening in friction stir welded joints.

$$\sigma = K\varepsilon^{n} \tag{1}$$

Where,

σ = Tensile Strength (MPa)

K = Strength Coefficient (MPa)

ε = Strain

n = Strain Hardening Exponent

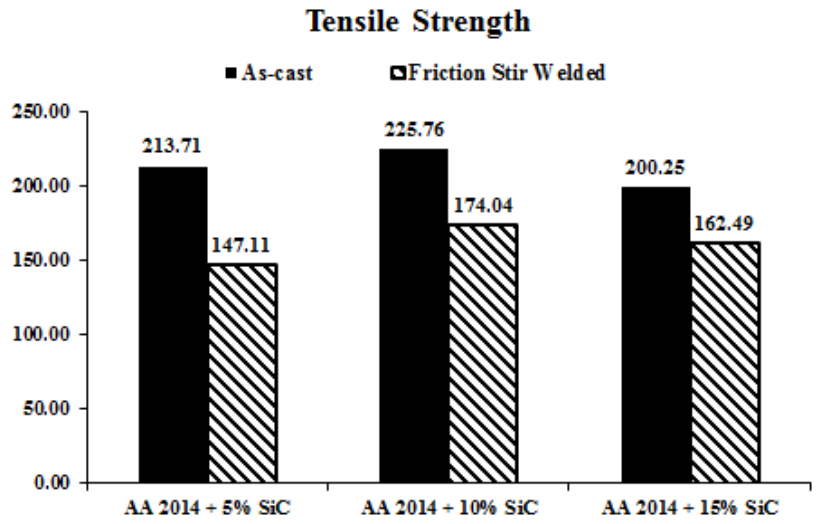

Figure 5.11 Plot of tensile strength of as-cast and friction stir welded composite

From Figure 5.12, it can be observed that the location of failure for all the welded composites was either from the as-cast region or HAZ. This indeed indicates higher strength of WN compared to other zones. Previously, Bozkurt et al. (2011) also reported similar observations. As reported earlier, that the stirring action generated by the tool leads to the homogenization and redistribution of SiC particles in the WN of composites (Marzoli, Strombeck, Dos Santos, Gambaro, & Volpone, 2006; Feng, Xiao, & Ma, 2008). Also, due to the uniform stirring action generated by the rotating tool, inter-particle spacing of SiC particles will decrease. Due to this, the content of fine size SiC particles will increase in WN. FSW process not only breaks the agglomeration present in as-cast composites but also closes the porosity and voids present in as-cast composites. Owing to these reasons, the strength of the WN will be comparatively higher than in other zones. Thus, HAZ, TMAZ or as-cast region becomes the prone zone for failure to take place. As discussed earlier in Figure 5.6 and Figure 5.7, HAZ and TMAZ were found to have higher defects and porosity when compared to WN. These voids and porosities will act as a weak zone and will promote crack propagation during tensile testing. Apart from this, WN of welded composites was found to have comparatively lower grain size. According to the Hall-Petch relationship, generation of finer grain size will ultimately enhance the load bearing capacity and thus improves mechanical properties. As discussed earlier, the variation in the HAZ is only due to thermal histories experienced by the material during the welding process. These thermal histories have a tendency to dissolve the strengthening precipitates present in composite material. As a result of this, the tensile strength of welded composites reduces significantly in comparison to that of as-cast composites. Similar results were also observed by other researchers (Bozkurt, Uzun, & Salman, 2011; Ceschini, Boromei, Minak, Morri, & Tarterini, 2007b; Ceschini, Boromei, Minak, Morri, & Tarterini, 2007a; Ni, Chen, Xiao, Wang, & Ma, 2014).

An increase in the weight percentage of reinforcement particles will restrict the flowability of the aluminium matrix and reduce the content of the ductile aluminium alloy in the resulting as-cast composite. This will adversely affect the percentage elongation of composites. The observed percentage elongation of welded composites along with percentage elongation of as-cast composites is shown in Figure 5.13. From Figure 5.13, it can be observed that with the increase in weight percent of reinforcement particles, the percentage elongation of welded composites decreases. In other words, the increase in weight percent of SiC particles tends to increase the brittleness. It is a known fact that

intensive stirring and extensive plastic deformation generated during the FSW process leads to grain refinement in WN. The grain boundaries act as major hurdles to the movement of dislocation. As a result of grain refinement, the number of grain boundaries per unit volume in the WN will be larger. Due to this, the percentage elongation of welded composites is lower than the corresponding percentage elongation of as-cast composites.

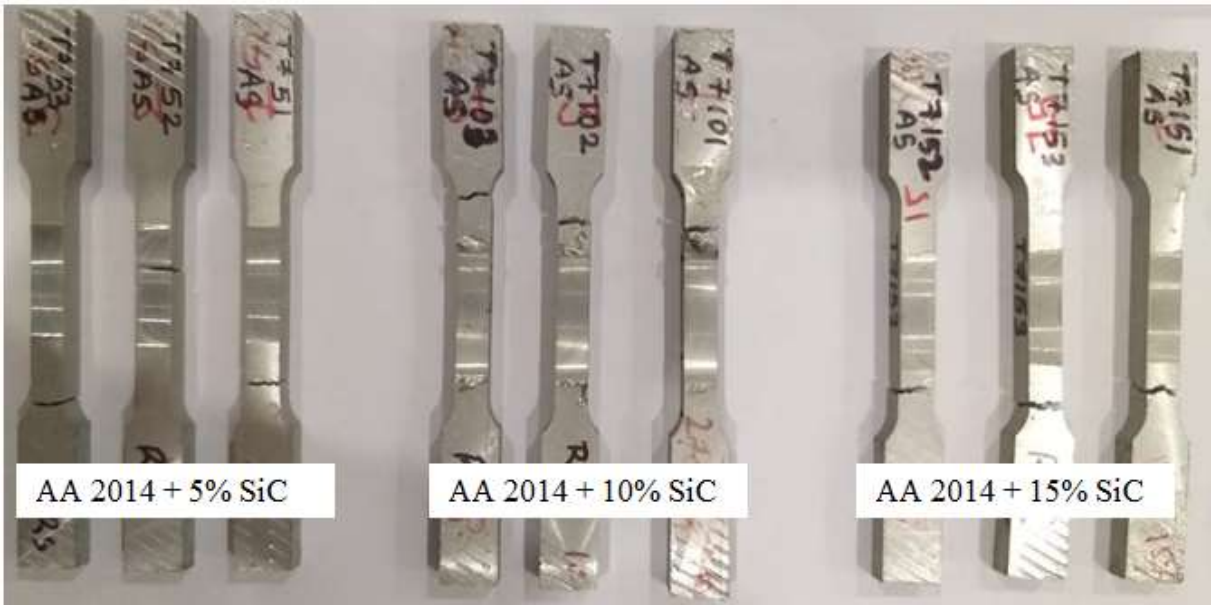

Figure 5.12 Friction stir welded specimens after performing a tensile test

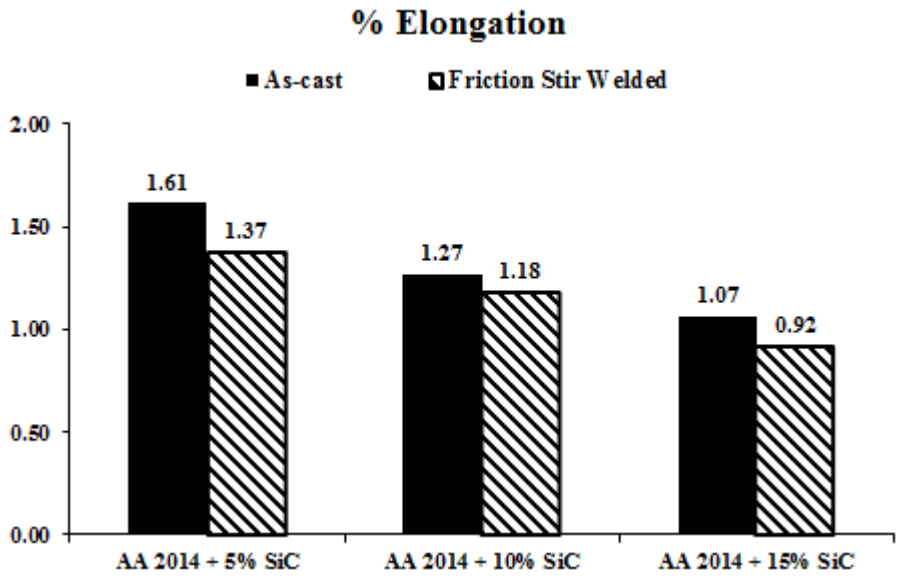

Figure 5.13 Plot of % elongation of as-cast and friction stir welded composite

5.7 Microhardness of Welded Composite

The plot of Vicker's microhardness of welded composites is shown in Figure 5.14. In order to understand the softening or hardening effects caused during the FSW process, the indentation for measurement of microhardness was performed from the as-cast region to the WN region. From Figure 5.14, it can be observed that the microhardness of welded composites increases with the increase in weight percent of reinforcement particles. The obvious reason for this observation is the hard nature of ceramic particles present in the matrix of aluminium alloy. With reference to AA 2014 + 5% SiC, it can be witnessed that microhardness tends to increase from the as-cast region to HAZ further progressing to TMAZ and finally attain the highest value in WN on the advancing side. However, the rate of increase in microhardness in the WN was comparatively higher. Apart from this, on the retreating side, it can be observed that microhardness decreases from WN to TMAZ and then slightly increase in HAZ and as-cast region. The microhardness of welded AA 2014 + 10% SiC and AA 2014 + 15% SiC, follows almost the same trend. With reference to the advancing side of these two composites, a continuous reduction in microhardness can be observed from the as-cast region to TMAZ and then after, microhardness increases and attains a maximum value in WN. However, on the retreating side, sharp reductions in microhardness can be observed in TMAZ and then after it increases in HAZ and as-cast region. The reason for lower microhardness in the HAZ or TMAZ is the void and porosity that were previously observed in Figure 5.6 and Figure 5.7. Also, it should be noted that the tensile specimens had failed from either of these zones.

The average microhardness in as-cast region of AA 2014 + 5% SiC, AA 2014 + 10% SiC and AA 2014 + 15% SiC were 95.16 Hv, 123.68 Hv and 133.36 Hv which was found to increase and attain a value of 127.2 Hv, 140.12 Hv and 150.19 Hv in WN of respective composites. This higher hardness of WN is attributed to the grain refinement, breaking in the agglomeration of reinforcement particles, homogenous distribution of reinforcement particles and defect free microstructure. Previously, other researchers also observed higher microhardness in weld nugget compared to that of as-cast composites (Feng, Xiao, & Ma, 2008; Ni, Chen, Wang, Xiao, & Ma, 2013; Nami, Adgi, Sharifitabar, & Shamabadi, 2011; Amirizad, et al., 2006).

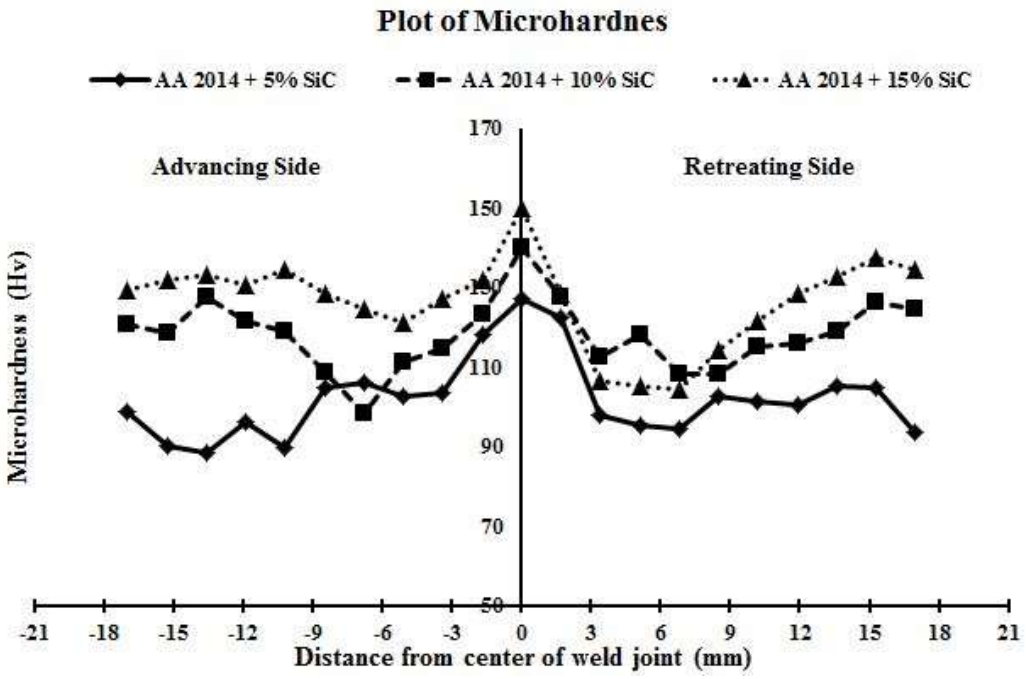

Figure 5.14 Plot of microhardness of friction stir welded composite

5.8 Summary

The present chapter demonstrates a successful attempt of welding AMC using the FSW process. The welding of as-cast composites was performed at a rotational speed of 270 rpm, welding speed of 78 mm/min and constant tool tilt angle of 2°. The effect of weight percent of reinforcement particle on microstructure and mechanical properties of welded composites can be summarized as follows:

- Based upon the thermal histories and deformation experienced by the material, all the welded composites revealed three different zones i.e. HAZ, TMAZ and WN. The microstructure of HAZ was almost similar to that of the as-cast region. However, with the increase in weight percent of reinforcement particles, defects were found to increase in HAZ and TMAZ of welded composites. It should be noted that TMAZ of all welded composites revealed comparatively higher welding defects such as voids and porosity when compared to HAZ. The microstructure of TMAZ revealed the presence of elongate grains which were oriented towards WN. Irrespective of the weight percent of reinforcement particles, WN revealed a refined grain structure with minimum welding defects. It was observed that a higher weight percent of reinforcement particles restricts the flow of plasticized material and offers resistance towards the rotating tool. As a

result of this, the larger size of SiC particles along with particles free region was observed in the microstructure of welded AA 2014 + 15% SiC composite.

- With respect to as-cast composites, the tensile strength of welded composites revealed a noticeable reduction. The reduced tensile strength of welded composite still follows a similar trend as observed for tensile strength of as-cast composites. In comparison to as-cast composites, the tensile strength of welded composites reduces by 31.16%, 22.90% and 18.85% for AA 2014 + 5% SiC, AA 2014 + 10% SiC and AA 2014 + 15% SiC respectively. The possible reason for the reduction in tensile strength is the over-ageing of AA 2014 induced due to friction heat generated during the welding process. This will ultimately increase the strain hardening exponent in the weld joint. Lastly, it was observed that with the increase in weight percent of reinforcement particles, a reduction in elongation was observed. Also, the elongation of welded composites was comparatively lower than that of as-cast composites.
- With the increase in weight percent of reinforcement particles, the microhardness of welded composites was found to increase. Irrespective of the weight percent of reinforcement particles, the higher hardness was observed for WN and the lowest hardness was either reported in the as-cast region or in HAZ/TMAZ. The microhardness in as-cast region of AA 2014 + 5% SiC, AA 2014 + 10% SiC and AA 2014 + 15% SiC were 95.16 Hv, 123.68 Hv and 133.36 Hv. This hardness was found to increase and attain a value of 127.2 Hv, 140.12 Hv and 150.19 Hv in WN of respective composites.